Morphological changes associated with Nile crocodile (*Crocodylus niloticus*) phallic glans inflation

Brandon C. Moore [1,2], Rachel Francis[2], Adam Foster[2], Diane A. Kelly[3], Mark Does[4], Dong K. Kim[4], Herman B. Groenewald[5], Jan G. Myburgh[6]

[1] College of Veterinary Medicine, Department of Biomedical Science, University of Missouri, Columbia, Missouri

[2] Biology Department, Sewanee: The University of the South, Sewanee, Tennessee

[3] Psychological and Brain Sciences, University of Massachusetts, Amherst, Massachusetts

[4] Department of Biomedical Engineering, Vanderbilt University School of Medicine, Nashville, Tennessee

[5] Department of Anatomy and Physiology, Faculty of Veterinary Science, University of Pretoria, Onderstepoort, South Africa

[6] Department of Paraclinical Sciences, Faculty of Veterinary Science, University of Pretoria, Onderstepoort, South Africa

*Correspondence Brandon C. Moore, College of Veterinary Medicine, Department of Biomedical Science, University of Missouri, Columbia, MO 65211. Email: bcmoore@missouri.edu

Funding information: University of Pretoria

Abstract

The crocodylian phallic glans is the distal inflatable structure that makes the most direct contact with the female cloacal and associated reproductive tract openings during copulation. Therefore, its form and function directly impact female tissue sensory interactions and insemination mechanics. Compared to mammals, less is known about glans functional anatomy among other amniotes, including crocodylians. Therefore, we paired an *ex vivo* inflation technique with magnetic resonance imaging 3D-reconstructions and corresponding histological analyses to better characterize the morphological glans restructuring occurring in the Nile crocodile (*Crocodylus niloticus*) at copulation. The expansion of contiguous inflatable spongiform glans tissues is variably constrained by adjacent regions of dense irregular collagen-rich tissues. Therefore, expansion shows regional differences with greater lateral inflation than dorsal and ventral. Furthermore, this enlargement elaborates the cup-like glans lumen, dorsally reorients the glans ridge, stiffens the blunt and bifid glans tip, and putatively works to seal the ventral sulcus spermaticus semen conduit groove. We suggest how these dynamic male structures may interact with structures of the female cloacal urodeum and how these morphological changes, in concert with the varying material properties of the structural tissue compartments visualized in this study, aid copulatory gamete transfer and resulting fecundity.

Research Highlights

- Nile crocodile glans inflation produces a reproductively relevant copulatory structure directing insemination and female tissue interactions.

- Pairing magnetic resonance imaging 3D reconstruction with corresponding histology effectively studies functional anatomy.

1 INTRODUCTION

Although amniote phalli share homologous embryonic origins, morphogenetic processes, and molecular genetic mechanisms associated with early development (Brennan, 2016a; Gredler, 2016), their adult morphologies across major amniote lineages are quite diverse (Eberhard, 2010). Three lineages, turtles (Kelly, 2004; McDowell, 1983; Zug, 1966), crocodylians (Johnston et al., 2014; Moore, Spears, Mascari, & Kelly, 2016; Otaño, Imhof, Bolcatto, & Larriera, 2010; Tavalieri et al., 2019; Ziegler & Olbort, 2007), and mammals (Akbari, Babaei, & Goodarzi, 2018; Baskin et al., 2018; Comelis, Bueno, Góes, Taboga, & Morielle-Versute, 2018; Cunha et al., 2014; Phillips, Wright, Gradie, Johnston, & Pask, 2015), have conspicuous glans structures on the distal phallus. In these taxa, the glans contains inflatable spongiform tissues that expand during sexual arousal and change the overall shape of the distal penis. It is probable that glans morphology plays a role in sexual selection, as in each lineage the glans shows significant inter-species shape differences, sometimes even (or especially) in closely related sister taxa (Eberhard, 1985). These differences are relevant because the glans is in a position to directly interact with terminal portions of the female reproductive tract during copulation, so may have the ability to increase male reproductive success through a range of mechanisms such as producing a male–female genital lock to improve sperm transfer, or stimulating the female to induce morphological and physiological changes conducive to conception (Brennan, 2016b). The specifics of many male–female tissue interactions during copulation remain unknown, but it has been hypothesized that they could produce selective pressures that can drive the rapid evolution of male glans form and function and its coevolution with female characteristics (Brennan, 2016b; Firman, Gasparini, Manier, & Pizzari, 2017; Sloan & Simmons, 2019).

Glans structures among vertebrates are likely to share a number of functional similarities related to producing specific and repeatable shapes, such as extensible tissues and elements that locally restrict expansion (Kelly, 2016). Glans anatomy has been generally described for mammals, where it is typically an inflatable, cap-shaped expansion of the corpus spongiosum found at the distal end of the penis (Jubilato et al., 2019; Weiss et al., 2012), but it is more poorly understood for other amniote taxa. Studies of the male turtle reproductive anatomy have, until recently, focused on the gross morphologies of noncopulatory glans, not characterizing glans inflation, internal structures, or histological details (Fernandes Araujo Chaves, Viana, Chaves, Miglino, & de Sousa, 2020; Gradela et al., 2019; Larkins & Cohn, 2015; Zug, 1966). Additional comparative studies are required to better define the anatomy and function of glans tissues across amniotes. Crocodylians have inflatable glans tissues that share gross similarities to those of mammals, and a detailed study of glans development in the American alligator (*Alligator mississippiensis*) has shown that the structure contains homologous, but nonidentical anatomical elements (Gredler, Seifert, & Cohn, 2015). Adult crocodylian glans tissues receive blood for inflation from bilateral vascular conduits that run from vascular tissues adjacent to the proximal phallic crurae to distal inflatable spongiform tissues, most notably through paired blood conduits that flank the ventral sperm-conducting sulcus spermaticus. This morphology has been described in alligators (Moore & Kelly, 2015; Moore et al., 2016), crocodiles (Moore, Groenewald, & Myburgh, 2020), and *Tomistoma* (Moore, Fitri, & Augustine, 2020), representing all three modern crocodylians lineages, and suggesting that the anatomical *Bauplan* related to inflation is ancestral to the group.

When pressurized fluid is experimentally directed through these conduits via syringe, it expands the glans spongiform tissues (Moore, Groenewald, et al., 2020) into a species-specific reproductive morphology. The general features of erect glans morphology in both alligators and crocodiles include a cup-like shape with an expanded distally-facing glans lumen, a prominent ridge dorsal to the ventrally-placed sulcus spermaticus, and an extension of the sulcus groove beyond the termination of the glans body termed the glans tip (Fitri et al., 2018; Johnston et al., 2014).

Histological studies, American alligators (Moore et al., 2016), Nile crocodiles (Moore, Groenewald, et al., 2020), Tomistoma (Moore, Fitri, et al., 2020), and broad-snouted caimans (Tavalieri et al., 2019) have shown that the boundaries of the inflatable spongiform cavities are reinforced by collagen and elastin fiber matrixes. However, a more descriptive, visual understanding of how the three-dimensional external and internal glans anatomy changes with inflation is lacking. Magnetic resonance imaging (MRI) allows nondestructive, high-contrast resolution, serial scanning of soft phallic tissues and clinical investigation of internal anatomy (Altun, 2019; Ozbey & Kumbasar, 2017). This technique can also be utilized *ex vivo* to study experimental animals and generate detailed volumetric reconstructions before serial histological sectioning and 2D-cellular analysis (Phillips et al., 2015). Flaccid and inflated 3D-glans models can be paired with corresponding histology to operate as a framework to investigate male–female reproductive function (Cunha & Baskin, 2018). We have previously presented a histological investigation comparing the flaccid and artificially inflated Nile crocodile (*Crocodylus niloticus*; Laurenti, 1768) glans (Moore, Groenewald, et al., 2020). Here, we use serial MR-images of four of those phalli to digitally reconstruct 3D-models of external and internal structures and compare flaccid and inflated glans morphology.

2 METHODS

Crododylus niloticus (Laurenti, 1768) phalli were collected at the Le Croc breeding farm and tannery near Brits, South Africa, May 2016. Animal handling and tissue collection procedures conformed to South African export (CITES certificates #10873 & 26376) and United States import (CITES schedule II) permitting and utilized University of Pretoria Institutional Animal Care and Use Committee (IACUC; project #V017-16) approved protocols. Necropsy of male carcasses occurred soon after routine farm slaughter. In total, 15 phalli were dissected and 7 of those glans were inflated, as detailed below. The associated gross anatomy and histological analyses have been presented previously (Moore, Groenewald, et al., 2020). We performed MRI analysis and subsequent 3D-reconstructions of this study on four specimens (snout-vent lengths 93–96 cm; age ~ 3.0 years). The glans was removed from intact phalli by transecting with scalpel mid-shaft between the beginning of the glans and the crura and immersed in 10% neutral buffered formalin (NBF) either in its flaccid state or after artificial glans inflation ($n = 2/2$). Glans tissues were inflated by inserting a 10 ml syringe fitted with a 21-gauge needle into one of the two blood vessels flanking the sulcus spermaticus at the cut proximal end of the tissue (Moore, Groenewald, et al., 2020). Subsequently, the bisected end of the tissue with inserted needle was tightly ligated with twine to impede fluid backflow through the contralateral blood vessel or other conduits. NBF was injected into the spongiform tissues of the glans using sufficient constant pressure to cause inflation. When the tissue reached a maximum size, the syringe was held under compression for a few minutes to maintain internal pressure while the fixative crosslinked the expanded tissues, thus maintaining the enlarged shape. Following inflation, the whole glans was immersed in NBF for further fixation.

Each glans was washed in ×1 phosphate-buffered saline before imaging in a Bruker Biospec MRI scanner using a 72 mm diameter Bruker volume RF coil and a 3D-FLASH sequence (T/TR/Flip/NA = 6.5 ms/25 ms/14°/2) and a total scan time ~ 2 hr. Axial images were 125 × 125 μm isotropic resolution while coronal and sagittal images were 500 x 125 mm^2. The MRI quality of each sample was equivalent and the images shown in each figure are comparable across samples.

After imaging, each glans was prepared using standard histological paraffin techniques and serial sectioned at 7 μm in the transverse plane. Slides were stained with either Milligan's trichrome with aniline blue resulting in blue collagen, red nuclei, and red/purple muscles; or Weigert's resorcin fuchsin resulting in purple elastin fibers with nuclear fast red counterstaining. Analysis of these histological data has been published elsewhere (Moore, Groenewald, et al., 2020), but they were used here to confirm the identification and configuration of specific tissue types in corresponding MRI transverse sections.

Each MRI transverse image stack was imported into BioVis3D (Montevideo, Uruguay) and the outlines of six tissue types/compartments were manually traced and color coded as follows: epithelium/pink, dense collagen fiber-rich connective tissue/blue, elastin fiber-rich connective tissue/green, spongiform tissue/purple, smooth muscle fiber bundle regions/yellow, and the sulcus spermaticus/red. The traces were compiled into the digital reconstructions presented here. Each pair of flaccid and inflated 3D-reconstructions was compared to determine agreement among each morphological feature discussed below.

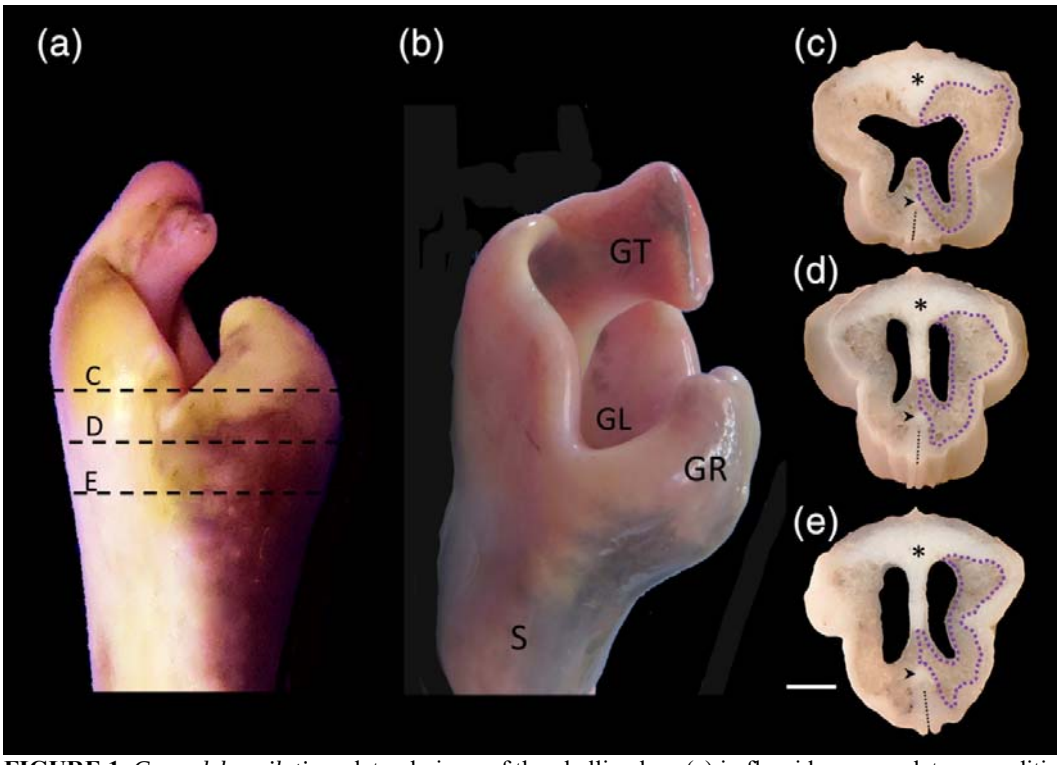

FIGURE 1. *Crocodylus niloticus*, lateral views of the phallic glans (a) in flaccid, noncopulatory condition and (b) after artificial inflation technique to copulatory state showing the glans ridge (GR), glans lumen (GL), glans tip (GT), and shaft (S). The sulcus spermaticus is out of view to the left in both images. (c–e) Gross cross-sections of glans corresponding to dashed line planes denoted respectively in (a) revealing spongiform tissues highlighted in hemi section with purple dotted lines and the locations of dense collagen tissues marked dorsally with asterisks and also superior to the ventral sulcus spermaticus (short dotted lines) with arrowheads. Scale bar = 5 mm

3 RESULTS

The glans of *Crocodylus niloticus* expands in multiple dimensions as blood enters and inflates the spongiform tissues within (Figure 1c–e). Across samples, the tissue expansion, in turn, increased the glans lumen volume, changed the shape and position of the glans ridge, and broadened the lateral faces of its distal cup (compare Figure 1a,b). The expandable portion of the glans effaces and mechanically interacts with the dense collagen-rich connective tissues found throughout the phallic shaft, the dorsal glans ridge, and the area superior to the sulcus spermaticus (Figure 1c-e).

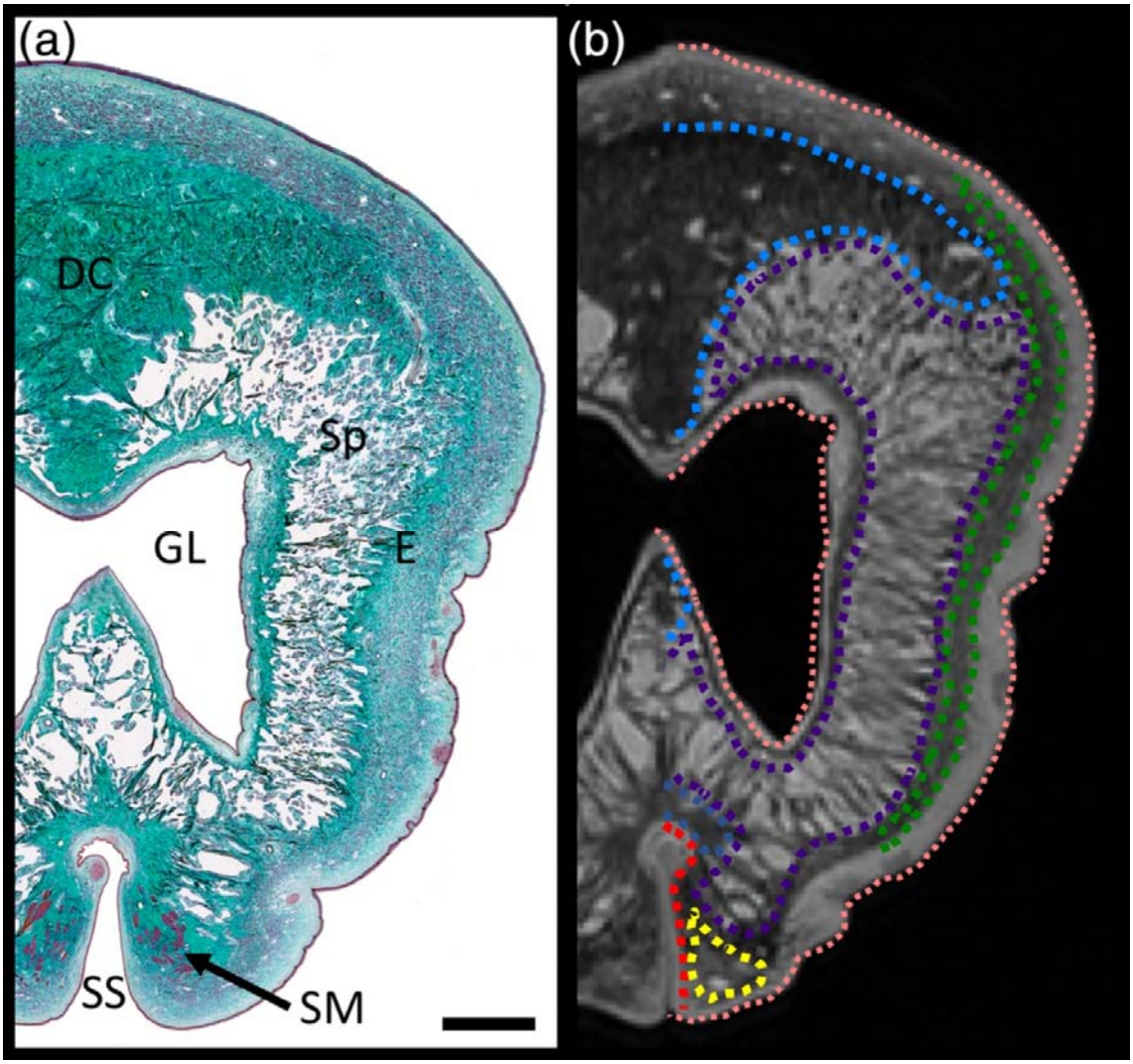

FIGURE 2. *Crocodylus niloticus*, correspondence between medial glans tissue compartment histological staining and MRI. (a) Milligan's trichrome section: glans lumen (GL), dense collagen tissue (DC), spongiform tissue (Sp), elastin-rich tissues (E), sulcus spermaticus (SS) note the groove opening is a histological processing artifact, smooth muscle fiber bundles (SM). Scale bar = 2 mm. (b) MRI dotted line traces: epithelia (pink), dense collage tissues (blue), spongiform tissues (purple), elastin-rich tissues (green), sulcus spermaticus (red), and smooth muscle fiber bundles (yellow). See also supplemental online material Figure S1 for additional correspondence images

MRI of artificially inflated glans tissues yielded segments that clearly correspond to stained tissues in histological sections (medial glans: Figure 2a,b; proximal glans: supplemental online material, Figure S1a,b). Dense, irregular collagenous regions were readily apparent as darker areas in the MRI images. Although spongiform erectile tissue is also collagenous, expansion of its vascular tissue reduces its overall density so it appears lighter and striated in MR-imaging. Identifying elastin fiber-rich areas in the MR-images was less straightforward, and we depended on correlating digital images with corresponding histologically sectioned tissue stained for elastin with Weigert's resorcin fuchsin to confirm distributions.

The morphological effects of inflation on tissues inside the glans become apparent when we compare sequential transverse flaccid and inflated tissue MR-images at analogous planes (Figure 3). The phallic shaft is relatively unchanged by inflation beyond the expansion of sulcus-adjacent blood vessels and spongiform tissues that laterally compress both more medially located smooth muscle regions and the sulcus groove (Figure 3a,b). Proximally, inflatable tissues are found adjacent to the sulcus; more distally they make up a larger proportion of the glans volume, filling areas lateral to the medially placed, irregular collagen fiber-rich connective tissues. At the point where the phallic shaft shifts to glans, the cross-section of the central mass of dense collagenous tissue changes from the crescent-shape characteristic of the phallic shaft to a laterally compressed “mushroom” shape flanked by spongiform tissues that is, in turn, laterally bounded by elastin-rich tissue layers under the epithelia (Figure 3c-f). Sagittal (Figure 6b,c) and longitudinal (Figure 7b,c) MR-images of the inflated glans show that in this region the dense collagen fiber-rich tissues form paired indentations in their distomedial aspect that interdigitate with and support the more distal spongiform tissues (Figure 7a,b).

Morphological changes in medially placed, irregular collagen fiber-rich connective tissues in more distal regions of the phallus widen the flaccid glans dorsally and narrow it ventrally (Figure 3c,e), but the lateral expansion of erectile tissues during inflation increases the lateral glans width (Figure 3d,f). Potential dorsoventral expansion during inflation is restricted by a broad mass of dense collagenous tissue that underlies the glans ridge (Figure 3e,f).

Further distally, the glans ridge with its subjacent inflatable tissues that run under the dense collagen shield diverges from the lateroventral portion of the glans (Figure 3g,h). This upper/lower split is observed at the notch observable on each lateral glans face (Figure 1e). The glans ridge diminishes in diameter distally, but maintains the pattern of inflatable tissue ventral to denser tissue until reaching termination (Figure 3i,j). The remainder of the glans becomes a W-shaped segment of inflatable tissues that carry the sulcus spermaticus medioventrally. Inflating these tissues produces both lateral expansion of the ventral glans and expansion of tissues around the sulcus. Erectile tissues extend into the glans tip (Figure 3k,l), where tissue diameter decreases distally until the tip ends in a blunt, hooked bifid termination (Figure 1e). Concomitantly, the distal portion of the sulcus spermaticus becomes shallower and the deepest aspect moves from a central position in the shaft to a more ventral placement in the glans tip (Figure 3a,b vs. i,j).

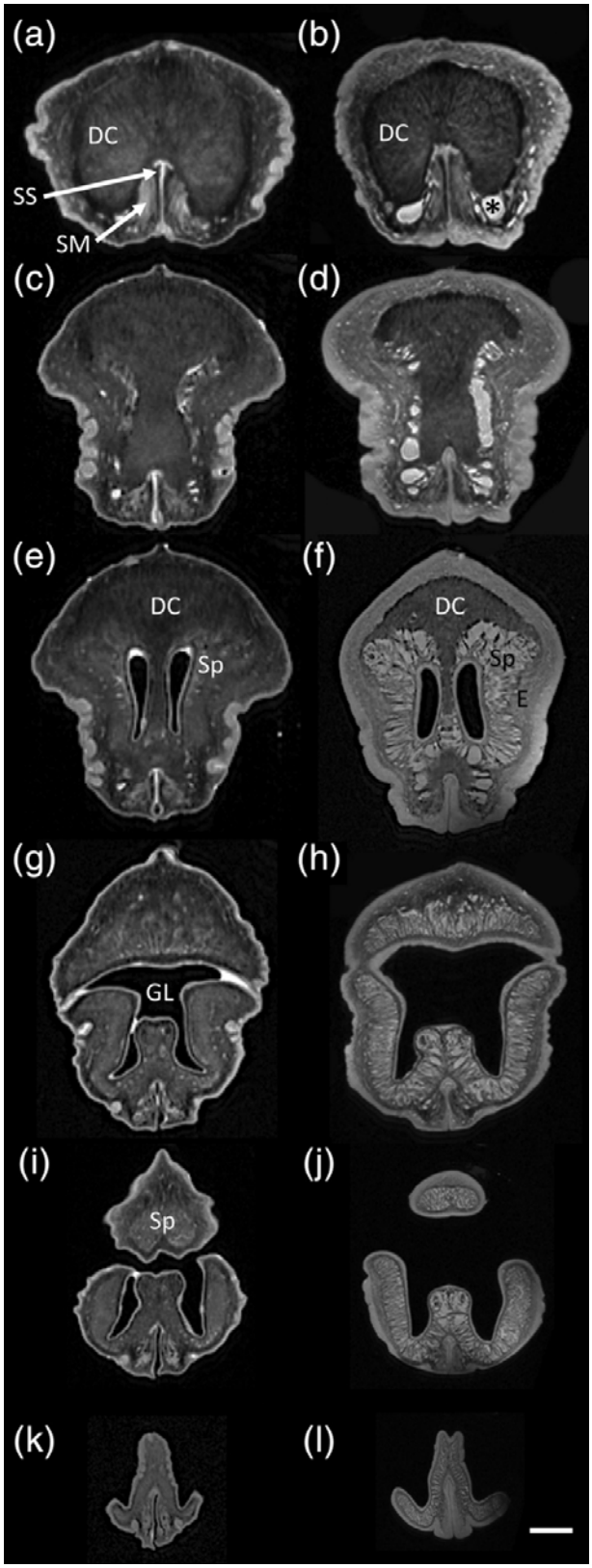

FIGURE 3. *Crocodylus niloticus*, serial MR-frames from flaccid (left column) and inflated (right column) crocodile glans progressing from proximal (top row) to distal (bottom row). Label abbreviations match those of Figure 2. The asterisk in B marks the location of the needle insertion to artificially inflate the spongiform glans tissues. Scale bar = 2 mm

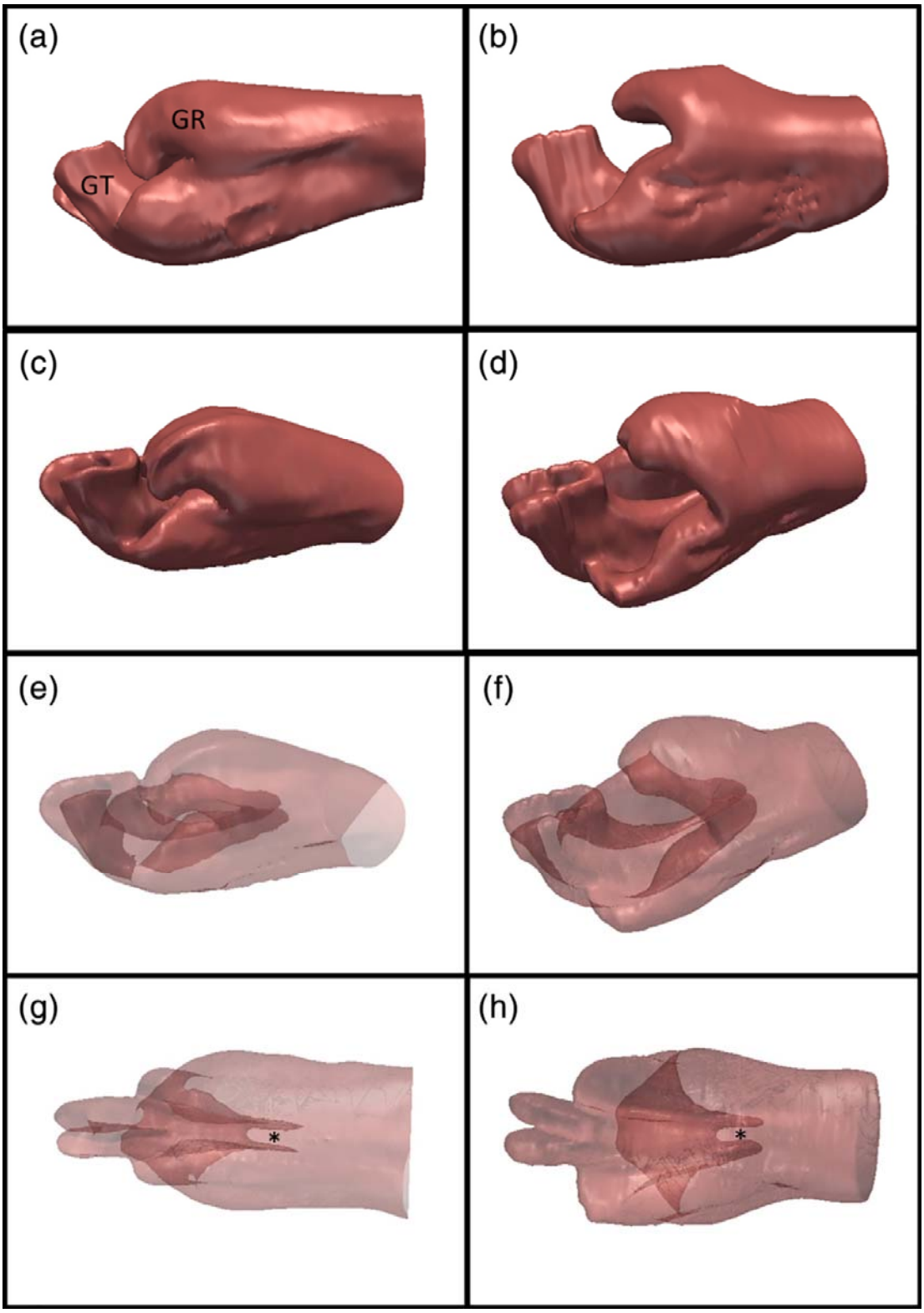

FIGURE 4. *Crocodylus niloticus*, 3D reconstructions of flaccid (left column) and inflated (right column) crocodile glans epithelia: glans ridge (GR) and glans tip (GT) based on MR-images. (a,b) Lateral views. (c,d) Laterodorsal oblique views. (e,f) Laterodorsal oblique, semitransparent views showing the volume glans lumens and the spaces within the bifid glans tips. (g,h) Dorsal, semitransparent view showing the bifid glans tip, the glans lumen sizes, and the placement of the vertical septum spanning the deep lumen (asterisks)

Inflation-derived changes in internal morphology alter the overall shape of the glans. In the flaccid *C. niloticus* glans, the terminus of the glans ridge is in close proximity to the glans tip and partially occludes the glans lumen (Figure 4a). Inflation reorients the glans ridge, raising it above the luminal space and increasing its distance from the tip (Figure 4b). As the lateral walls of the glans swell and flatten, the volume of the glans lumen increases: the cavity becomes wider and taller (Figure 4e,f) and the deepest aspect enlarges so that the vertical septum becomes visible (Figure 4c,d). The lumen does not expand proximally, as being constrained by the dense collagen connective tissue septum and flanking lateral curvatures (Figure 4g,h). The glans tip displays only modest lateral expansion, but after inflation its bifid terminus is more pronounced (Figure 4c,g vs. g,h).

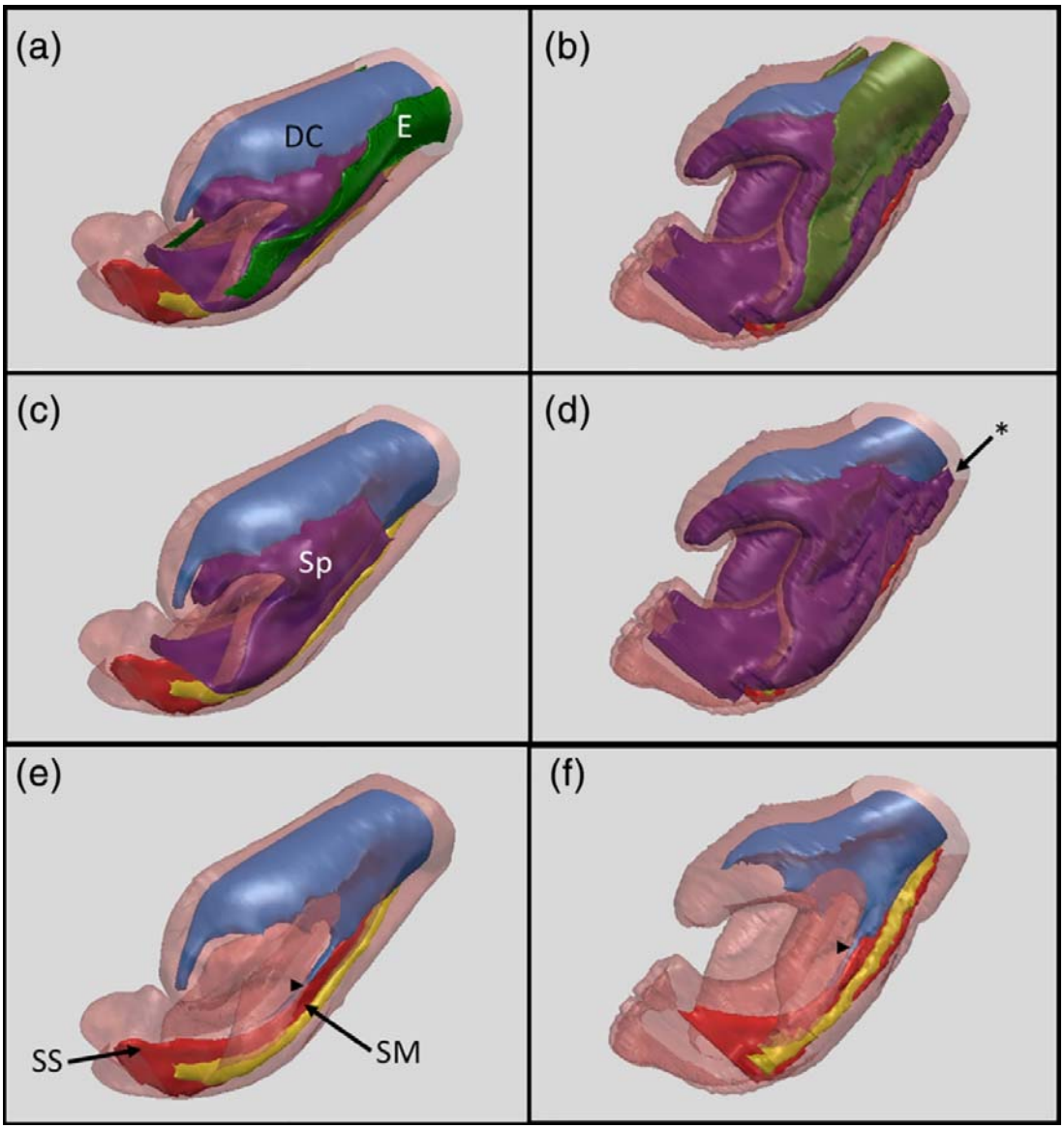

FIGURE 5. *Crocodylus niloticus*, 3D MRI reconstructions of flaccid (left column) and inflated (right column) crocodile glans internal structures in oblique view, based on MR-images. Label abbreviations and tissue compartment reconstruction colors match those of Figure 2. (a,b) All tissue compartments displayed. (c,d) Elastin-rich region omitted. The asterisk and arrow in D mark the needle insertion location to artificially inflate the spongiform glans tissues. (e,f) Elastin-rich and spongiform tissue regions omitted. Arrowheads mark a slender dense connective tissue process located dorsal to the sulcus spermaticus

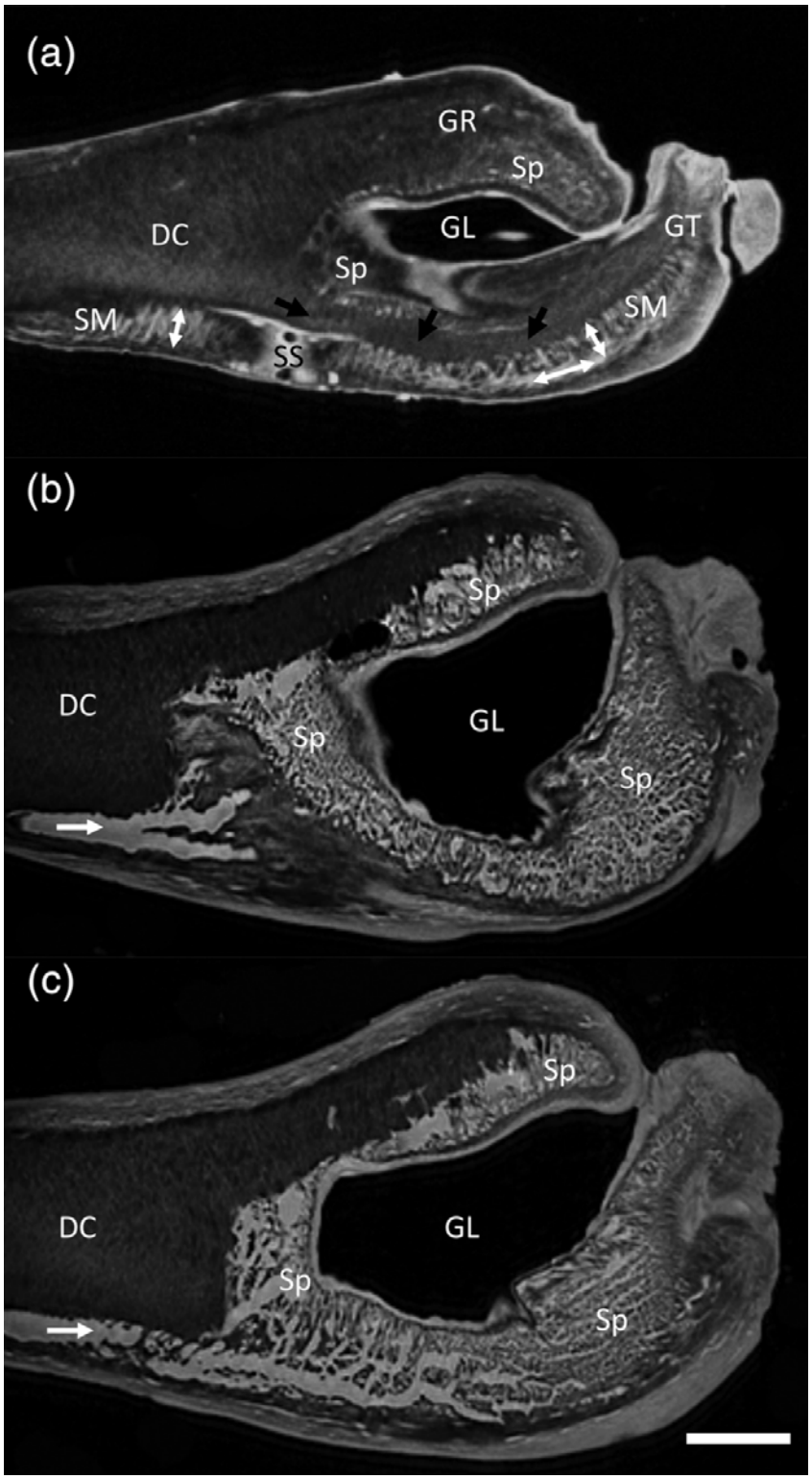

FIGURE 6. *Crocodylus niloticus*, glans sagittal MR-images: (a) flaccid and (b,c) inflated. Label abbreviations match those of Figure 2. (a) Medial plane image bisecting the sulcus spermaticus and flanking smooth muscles. Black arrows mark a slender, dense connective tissue process located dorsal to the sulcus spermaticus. White double headed arrows note the presence of both radial and longitudinal smooth muscle fiber bundle orientations. (b,c) Images progressing laterally from the medial sulcus plane showing ventrally placed vascular spaces branching at the initiation of the proximal glans (white arrows), radiating throughout the glans with numerous anastomoses, and infiltrating all spongiform, inflatable tissues. Scale bar = 5 mm

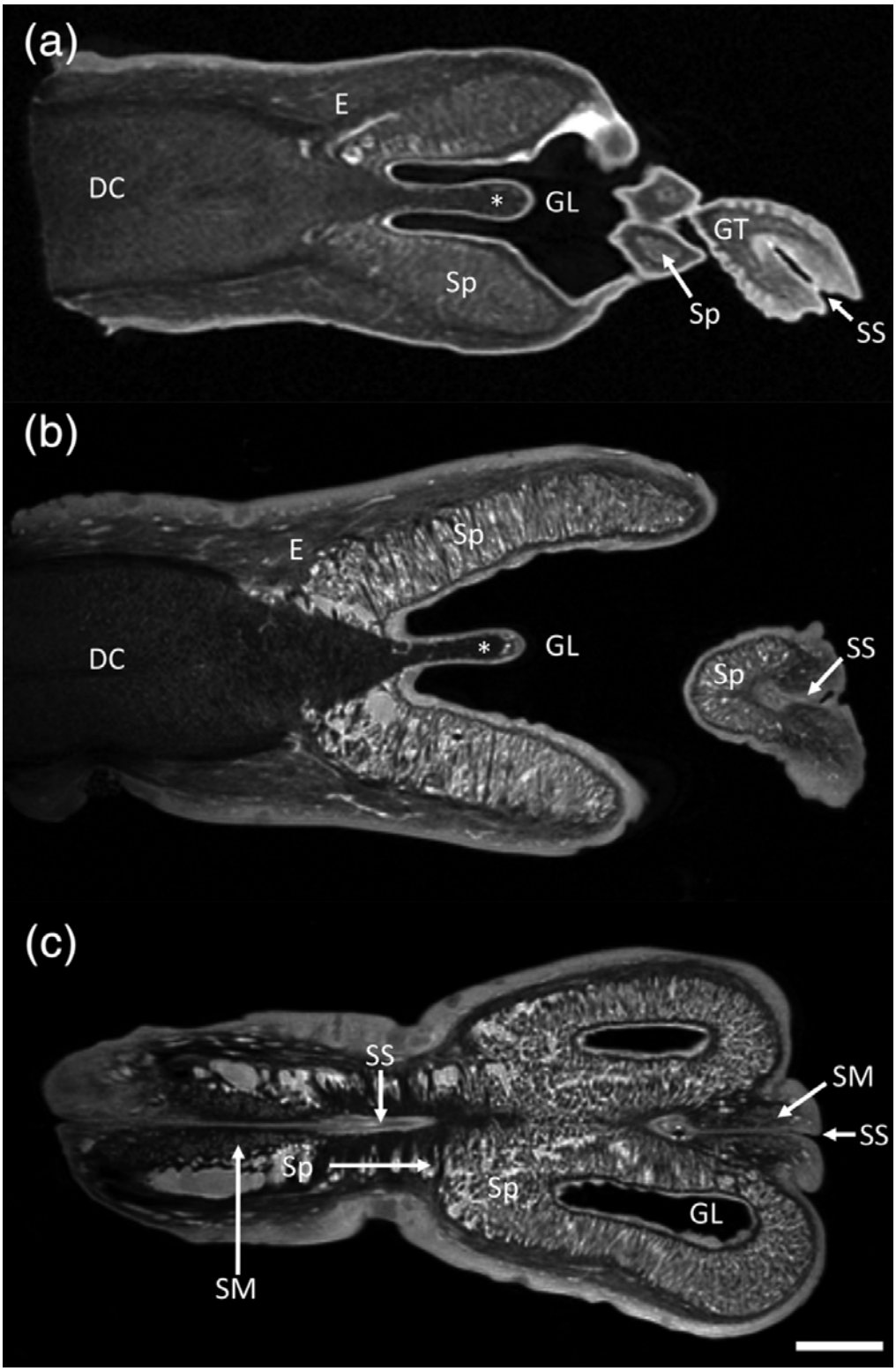

FIGURE 7. *Crocodylus niloticus*, glans coronal MR-images: (a) flaccid and (b,c) inflated. Label abbreviations match those of Figure 2. (a) A plane medial through the glans shows the extension of dense collagen connective tissues that comprise the vertical septum in the deep glans lumen (asterisk), the elastin-rich areas on the lateral faces of the glans, and how spongiform tissues extend to the terminus of the glans ridge. (b) Representative of the morphological change from image A occurring with glans inflation. (c) Ventrally oriented section plane showing the bi-lateral nature and continuity of spongiform tissues from the distal shaft on the left to the glans on right. Scale bar = 5 mm

The morphological remodeling described above occurs because specific tissue types within the phallus respond differently as fluid volume increases during inflation. MRI 3D reconstruction of specific tissue compartments in flaccid and erect phalluses show that while inflation increases collagenous erectile tissue volumes, their expansion is restricted dorsally and medially by masses of denser, noninflatable collagenous tissue (Figure 5a–d). Elastin fiber-rich tissue regions flank the glans laterally (Figures 2b, 5a,b, and 7a,b), these more extensible tissues facilitate the lateral expansion of erectile volumes. The inflatable tissues of the glans tip and the conduits to the inflatable glans tissues become more evident with artificial inflation in reconstructions (Figure 5c,d). The 3D models also highlight the filiform extension of dense connective tissue that projects from the shaft and overlies the sulcus spermaticus (Figure 5e,f).

Sagittal MRI also illustrates variations in smooth muscle fiber orientations found along the sulcus spermaticus length (Figure 5e,f). Fiber bundles adjacent to the deeper part of the sulcus are oriented radially, but the shallower parts of the groove are flanked by fibers with more longitudinal alignments (Figure 6a). This configuration seems to be most prominent in the medial to distal parts of the glans, as compared to the shaft and proximal glans where smooth muscle fibers are mostly oriented radially.

While the vasculature that carries blood through the phallic shaft to the spongiform tissues of the glans is not distinct in MRIs of flaccid tissue, they are evident in images from inflated tissue. Entering the glans, blood passes through bifurcating conduits running lateral to and parallel with the muscle masses flanking the sulcus spermaticus (Figure 6b) that subsequently expand into all of the distal spongiform tissues (Figure 6c). Images of the ventral portion of the glans in the longitudinal plane further show that spongiform erectile tissues in the glans are interconnected to form a single functional volume, such that fluid entering the space from a single phallic blood vessel can inflate the entire glans into its copulatory shape (Figure 7c).

4 DISCUSSION

Although we observed subtle differences in glans pigmentation pattern and size among individual crocodiles upon dissection, the subsequent transitions to the inflated glans shape was consistent and profound, characterized by increased glans height, width, and lumen volume, as well as tip engorgement (Moore, Groenewald, et al., 2020). Taken together, inflation produced an enlarged copulatory morphology that putatively seals the sulcus groove during semen transfer, shifts the positions of glans features, and increases overall rigidity, all of which produce a reproductively relevant structure for female cloacal interaction. Based on these and previous observations of crocodile glans morphology, as well as what is known about female cloacal anatomy, we can make investigable predictions about copulatory interactions.

Crocodylians typically copulate while at least partially submerged, which produces challenges for both intromission and insemination. Nile crocodiles have a three-dimensional aquatic copulatory repertoire that includes circling, rubbing, and submerging before male mounting and intromission (Garrick & Lang, 1977). While a male crocodylian's stiff, noninflatable phallic shaft facilitates initial intromission into the female vent (Kelly, 2013), subsequent movements of the pair such as rolls during copulation risk dislodging the male before insemination is completed. Upon inflation, the lateral glans expansion may help prevent the phallus from dislodging by interacting with female cloaca tissues to produce a “genital copulatory lock.” The dense collagen on the distal face of the shaft provides a large

surface area that interdigitates with and anchors to glans spongiform tissues, favoring outwardly directed lateral and vertical forces as the cup-like region of the glans expands during inflation. If muscles in the female uroproctodeal fold contract around the neck of the widened proximal glans, it could hold the distal end of the phallus close to the oviducal openings within the urodeum (Briggs-Gonzalez et al., 2017; Gist, Bagwill, Lance, Sever, & Elsey, 2008; Grigg & Kirshner, 2015; Johnston et al., 2014). Furthermore, the dense, vertically oriented connective tissues of the glans medial septum would act as a reinforcing skeletal element to resist compressive forces from the female.

Copulating underwater brings with it a risk that water from the environment could dilute or disrupt semen to a degree that would impede insemination or fertilization. Glans expansion fills space in the urodeum, which might displace existing water inside the cloaca and exclude further water intrusion from the external environment. At the ventral face of the Nile crocodile glans, the inflation of tissues flanking the centrally placed sulcus spermaticus expands the external edges of the sulcus spermaticus, effectively closing its superficial aspect and medially narrowing the open groove to form a tube. This ostensibly protects semen from water and waste products in the female's cloaca. Similar inflation changes have been reported in American alligators (Moore & Kelly, 2015). The compressive narrowing of the sulcus would also affect the transport dynamics of semen. Crocodiles do not have proximal muscles that drive semen in pressurized emissions as mammals do (Puppo & Puppo, 2016); instead, semen is moved steadily along the groove by peristaltic pressures from alternately contracting smooth muscles lateral to the sulcus groove (Johnston et al., 2014). We have shown evidence of orthogonally placed smooth muscles that could provide coordinated peristaltic semen propulsion.

While inflatable tissues seal the open ventral surface of the sulcus to the distal end of the glans tip, a dense filiform collagen extension of the phallic shaft is found superior to the deepest aspect of the sulcus along the length of the glans tip. Its position dorsally limits sulcus expansion when the spongiform tissues lateral to the sulcus expand during glans engorgement, and it could also prevent female muscular contractions from compressing the deep sulcus and potentially obstructing semen movement. (Moore and Kelly (2015) identified the deep sulcus as the main semen conduit in the American alligator.) This support structure is also elastin-rich (Moore, Groenewald, et al., 2020), so it may also store any energy of deformation to reposition the tip around the oviduct openings during copulation.

Glans inflation proceeds via the expansion of collagen and elastin-rich tissues in response to an influx of blood that increases spongiform tissue volume. Expansion is restricted as collagen fibers in the bounding tissue straighten and are loaded in tension (Kelly, 2007); the more extensible elastin fibers store energy that can assist tissue recoil during detumescence. Comparatively, abundant elastin fibers with similar function have been observed in the glans of American alligators (Moore et al., 2016), humans (Hsu et al., 1994), and rams (Schimming & Moraes, 2018). In the Nile crocodile, histological analysis showed that elastin fibers primarily overlie the lateral inflatable regions in distinct layers of both the inner and outer walls of the glans cup, but are thicker on its lateral (outer) walls (Moore, Groenewald, et al., 2020). Glans deflation is putatively benefical before phallic retraction back into the male vent after copulation, and may be facilitated by elastin elements.

While it is clear that shaft rigidity facilitates intromission and appropriate glans placement, little is known about the role(s) of the glans during insemination in the Nile crocodile. Assuming semen emission occurs at the most distal sulcus, the medial deflection of the glans

tip could help to direct ejaculate. Due to its comparatively large size and blunt form, we expect that during semen transfer the glans tip does not enter the female reproductive tract, but rests adjacent to the two small discrete female oviducal openings (Grigg & Kirshner, 2015). Alternatively, semen may not travel fully to the sulcus terminus and exit somewhere on the ventral glans. In both cases, more characterization of the crocodilian female cloacal urodeum, oviducal opening, and male/female positioning in intromission will be required for further understanding how these tissues interact during copulation.

Additionally, the functional role of the conspicuous glans ridge in insemination is also unclear. With a high dense collagen content contiguous with the collagenous tissues of the shaft, this area is less flexible than the lateral faces of the glans, and demonstratively changes position during inflation. During copulation the glans ridge would contact the dorsal urodeum wall and, as an extension of rigid shaft tissues, could either stabilize the glans position in the cloaca and/or transfer intromission forces to this surface. It is provocative to consider the lateral notches with less dense, more flexible underlying tissues act as hinge points that allow the phallus to flex during the application of copulatory forces. This action would move the glans tip dorsally in an arcing manner, possibly aiding semen placement or stimulating female tissues as submerged crocodiles work to maintain their copulatory position.

The pairing 3D-reconstruction from MR imaging with histology in this study was an effective technique for studying the internal anatomy of the crocodilian glans, and has the potential to be applied to other soft tissue structures to investigate homology and novelty across crocodylian species.

ACKNOWLEDGMENTS

The authors have no conflicts of interest to declare. This research was in part funded by a University of the South faculty research grant. Many thanks to Mr Stefan van As (managing director of Le Croc breeding farm and tannery) for his ongoing assistance with Nile crocodile research. This work was performed in collaboration with South African Crocodile Industry Association (SACIA) and Prof. Gerry Swan, Director of the Exotic Leather Research Centre (ELRC) of the University of Pretoria, South Africa.

AUTHOR CONTRIBUTIONS

Brandon Moore: Conceptualization; data curation; formal analysis; funding acquisition; investigation; methodology; project administration; resources; supervision; validation; visualization; writing-original draft; writing-review and editing. **Rachel Francis:** Formal analysis; methodology; visualization; writing-review and editing. **Adam Foster:** Investigation; methodology; validation; visualization; writing-review and editing. **Diane Kelly:** Formal analysis; methodology; visualization; writing-review and editing. **Mark Does:** Investigation; resources; visualization; writing-review and editing. **Dong kyu Kim:** Data curation; resources; visualization; writing-review and editing. **Herman Groenewald:** Investigation; methodology; resources; writing-review and editing. **Jan Myburgh:** Investigation; methodology; resources; writing-review and editing.

REFERENCES

Akbari, G., Babaei, M., & Goodarzi, N. (2018). The morphological characters of the male external genitalia of the European hedgehog (*Erinaceus europaeus*). *Folia Morphologica*, 77(2), 293– 300. https://doi.org/10.5603/FM.a2017.0098

Altun, E. (2019). MR imaging of the penis and urethra. *Magnetic Resonance Imaging Clinics of North America*, 27(1), 139– 150. https://doi.org/10.1016/j.mric.2018.09.006

Baskin, L., Shen, J., Sinclair, A., Cao, M., Liu, X., Liu, G., … Cunha, G. R. (2018). Development of the human penis and clitoris. *Differentiation*, 103, 74– 85. https://doi.org/10.1016/j.diff.2018.08.001

Brennan, P. L. R. (2016a). Evolution: One penis after all. *Current Biology*, 26(1), R29– R31. https://doi.org/10.1016/J.CUB.2015.11.024

Brennan, P. L. R. (2016b). Studying genital coevolution to understand Intromittent organ morphology. *Integrative and Comparative Biology.*, 56, 669– 681. https://doi.org/10.1093/icb/icw018

Briggs-Gonzalez, V., Bonenfant, C., Basille, M., Cherkiss, M., Beauchamp, J., & Mazzotti, F. (2017). Life histories and conservation of long-lived reptiles, an illustration with the American crocodile (*Crocodylus acutus*). *Journal of Animal Ecology*, 86(5), 1102– 1113. https://doi.org/10.1111/1365-2656.12723

Comelis, M. T., Bueno, L. M., Góes, R. M., Taboga, S. R., & Morielle-Versute, E. (2018). Morphological and histological characters of penile organization in eleven species of molossid bats. *Zoology*, 127, 70– 83. https://doi.org/10.1016/j.zool.2018.01.006

Cunha, G. R., & Baskin, L. (2018, September). Development of human male and female urogenital tracts. *Differentiation*, 103, 1– 4. https://doi.org/10.1016/j.diff.2018.09.002

Cunha, G. R., Risbridger, G., Wang, H., Place, N. J., Grumbach, M., Cunha, T. J., … Glickman, S. E. (2014). Development of the external genitalia: Perspectives from the spotted hyena (*Crocuta crocuta*). *Differentiation*, 87(1–2), 4– 22. https://doi.org/10.1016/j.diff.2013.12.003

Eberhard, W. G. (1985). Sexual selection and animal genitalia. *In Sexual Selection and Animal Genitalia.* https://doi.org/10.4159/harvard.9780674330702

Eberhard, W. G. (2010). Evolution of genitalia: Theories, evidence, and new directions. *Genetica*, 138(1), 5– 18. https://doi.org/10.1007/s10709-009-9358-y

Fernandes Araujo Chaves, L. P., Viana, D. C., Chaves, E. P., Miglino, M. A., & de Sousa, A. L. (2020). Reproductive morphophysiology of the male scorpion mud turtle (*Kinosternon scorpioides* Linnaeus, 1766) in captivity. *Veterinary Medicine and Science*, 1– 9. https://doi.org/10.1002/vms3.245

Firman, R. C., Gasparini, C., Manier, M. K., & Pizzari, T. (2017). Postmating female control: 20 years of cryptic female choice. *Trends in Ecology & Evolution*, 32(5), 368– 382. https://doi.org/10.1016/J.TREE.2017.02.010

Fitri, W.-N. N., Wahid, H., Rinalfi, P. T., Rosnina, Y., Raj, D., Donny, Y., … Malek, A. A. A. (2018). Digital massage for semen collection, evaluation and extension in Malaysian estuarine crocodile (*Crocodylus porosus*). *Aquaculture*, 483(October 2017), 169– 172. https://doi.org/10.1016/j.aquaculture.2017.10.026

Garrick, L. D., & Lang, J. W. (1977). Social signals and behaviours of adult alligators and crocodiles. *American Zoologist*, 17(February), 225– 239.

Gist, D. H., Bagwill, A., Lance, V., Sever, D. M., & Elsey, R. M. (2008). Sperm storage in the oviduct of the American alligator. *Journal of Experimental Zoology Part A: Ecological Genetics and Physiology*, 309(10), 581– 587. https://doi.org/10.1002/jez.434

Gradela, A., Pires, I. C., Faria, M. D., Matos, M. H. T., Costa, M. M., Souza, R. K. C., … Franzo, V. S. (2019). Morphology and biometry of the reproductive organs of adult males of *Trachemys scripta elegans* reared in São Paulo state, Brazil. *Pesquisa Veterinaria Brasileira*, 39(7), 538– 548. https://doi.org/10.1590/1678-5150-PVB-5848

Gredler, M. L. (2016). Developmental and evolutionary origins of the Amniote phallus. *Integrative and Comparative Biology*, 56(4), 694– 704. https://doi.org/10.1093/icb/icw102

Gredler, M. L., Seifert, A. W., & Cohn, M. J. (2015). Morphogenesis and patterning of the phallus and cloaca in the American alligator, *Alligator mississippiensis*. *Sexual Development*, 9(1), 53– 67. https://doi.org/10.1159/000364817

Grigg, G. C., & Kirshner, D. (2015). Biology and evolution of Crocodylians. *In Csiro Publishing.*, 52, 325– 349. https://doi.org/10.1146/annurev.ento.52.110405.091303

Hsu, G. -L., Brock, G., von Heyden, B., Nunes, L., Lue, T. F., & Tanagho, E. A. (1994). The distribution of elastic fibrous elements within the human penis. *British Journal of Urology*, 73(5), 566– 571. https://doi.org/10.1111/j.1464-410X.1994.tb07645.x

Johnston, S. D., Lever, J., McLeod, R., Oishi, M., Qualischefski, E., Omanga, C., … D'Occhio, M. (2014). Semen collection and seminal characteristics of the Australian saltwater crocodile (*Crocodylus porosus*). *Aquaculture*, 422–423, 25– 35. https://doi.org/10.1016/j.aquaculture.2013.11.002

Jubilato, F. C., Comelis, M. T., Bueno, L. M., Taboga, S. R., Góes, R. M., & Morielle-Versute, E. (2019). Histomorphology of the glans penis in Vespertilionidae and Phyllostomidae species (Chiroptera, Mammalia). *Journal of Morphology*, 280(12), 1759– 1776. https://doi.org/10.1002/jmor.21062

Kelly, D. A. (2004). Turtle and mammal penis designs are anatomically convergent. *Proceedings of the Royal Society B: Biological Sciences*, 271(SUPPL. 5), S293– S295. https://doi.org/10.1098/rsbl.2004.0161

Kelly, D. A. (2013). Penile anatomy and hypotheses of erectile function in the American alligator (*Alligator mississippiensis*): Muscular eversion and elastic retraction. *Anatomical Record*, 296(3), 488– 494. https://doi.org/10.1002/ar.22644

Kelly, D. A. (2016). Intromittent organ morphology and biomechanics: Defining the physical challenges of copulation. *Integrative and Comparative Biology*, 56(4), 705– 714. https://doi.org/10.1093/icb/icw058

Kelly, D. A. (2007). Penises as variable-volume hydrostatic skeletons. *Annals of the New York Academy of Sciences*, 1101, 453– 463. https://doi.org/10.1196/annals.1389.014

Larkins, C. E., & Cohn, M. J. (2015). Phallus development in the turtle *Trachemys scripta*. *Sexual Development*, 9(1), 34– 42. https://doi.org/10.1159/000363631

McDowell, S. B. (1983). The genus Emydura (Testudines: Chelidae) in New Guinea with notes on the penial morphology of Pleurodira. In Advances in herpetology and evolutionary biology (pp. 169– 183). Cambridge, MA: Museum of Comparative Zoology.

Moore, B. C., Fitri, W.-N., & Augustine, L. (2020). Crocodylian conservation and evolution insights from an anatomical and histological examination of phalli from male false gharial (*Tomistoma schlegelii*). *Anatomia, Histologia, Embryologia*, 1– 12. https://doi.org/10.1111/ahe.12542

Moore, B. C., Groenewald, H. B., & Myburgh, J. G. (2020). Histological investigation of the Nile crocodile (*Crocodylus niloticus*) phallic glans. *South American Journal of Herpetology* In Press.

Moore, B. C., & Kelly, D. A. (2015). Histological investigation of the adult alligator phallic sulcus. *South American Journal of Herpetology.*, 10(1), 32– 40. https://doi.org/10.2994/SAJH-D-14-00037.1

Moore, B. C., Spears, D., Mascari, T., & Kelly, D. A. (2016). Morphological characteristics regulating phallic glans engorgement in the American alligator. *Integrative and Comparative Biology.*, 56, 657– 668. https://doi.org/10.1093/icb/icw012

Otaño, N. B. N., Imhof, A., Bolcatto, P. G., & Larriera, A. (2010). Sex differences in the genitalia of hatchling *Caiman latirostris*. *Herpetological Review*, 41(1), 32– 35. Retrieved from. http://www.academia.edu/download/30591979/HR_March_2010_p32_35_Nunez.pdf

Ozbey, H., & Kumbasar, A. (2017). Glans wings are separated ventrally by the septum glandis and frenulum penis: MRI documentation and surgical implications. *Türk Üroloji Dergisi/Turkish Journal of Urology*, 43(4), 525– 529. https://doi.org/10.5152/tud.2017.00334

Phillips, T. R., Wright, D. K., Gradie, P. E., Johnston, L. A., & Pask, A. J. (2015). A comprehensive atlas of the adult mouse penis. *Sexual Development*, 9(3), 162– 172. https://doi.org/10.1159/000431010

Puppo, V., & Puppo, G. (2016). Comprehensive review of the anatomy and physiology of male ejaculation: Premature ejaculation is not a disease. *Clinical Anatomy*, 29(1), 111– 119. https://doi.org/10.1002/ca.22655

Schimming, B. C., & Moraes, G. N. (2018). Morphological analysis of the elastic and collagen fibers in the ram penis1. *Pesquisa Veterinaria Brasileira*, 38(11), 2166– 2174. https://doi.org/10.1590/1678-5150-PVB-5325

Sloan, N. S., & Simmons, L. W. (2019). The evolution of female genitalia. *Journal of Evolutionary Biology*, 32, 882– 899. https://doi.org/10.1111/jeb.13503

Tavalieri, Y. E. E., Galoppo, G. H. H., Canesini, G., Truter, J. C. C., Ramos, J. G. G., Luque, E. H. H., & Muñoz-de-Toro, M. (2019). The external genitalia in juvenile *Caiman latirostris* differ in hormone sex determinate-female from temperature sex determinate-female. *General and Comparative Endocrinology*, 273, 236– 248. https://doi.org/10.1016/j.ygcen.2018.10.003

Weiss, D. A., Rodriguez, E., Cunha, T., Menshenina, J., Barcellos, D., Chan, L. Y., … Cunha, G. (2012). Morphology of the external genitalia of the adult male and female mice as an endpoint of sex differentiation. *Molecular and Cellular Endocrinology*, 354, 94– 102. https://doi.org/10.1016/j.mce.2011.08.009

Ziegler, T., & Olbort, S. (2007). Genital structures and sex identification in crocodiles. *Crocodile Specialist Group Newsletter*, 26(3), 16– 17.

Zug, G. R. (1966). The penial morphology and the relationships of cryptodiran turtles. *Occasional Papers of the Museum of Zoology University of Michigan*, 647, 1– 24.